BAV Journal

2026 No. 108 ISSN 2366-6706

Bundesdeutsche Arbeitsgemeinschaft für Veränderliche Sterne e.V.

http://bav-astro.de

Secular period decrease and improved quadratic ephemeris of the eclipsing binary V804 And = MoV99

Reffke, Udo – Bad Zwischenahn, Germany
email: UR.Reffke@web.de

Bernhard, Klaus - Linz, Austria
email: Klaus1967Bernhard@gmx.at

Moschner, Wolfgang - Lennestadt, Germany
email: wolfgang.moschner@gmx.de

Frank, Peter - Velden, Germany
email: frank.velden@t-online.de

Bundesdeutsche Arbeitsgemeinschaft für Veränderliche Sterne e.V.

March 2026

Abstract

We present a long-term eclipse-timing analysis of the eclipsing binary V804 And (= MoV99) based on 67 CCD times of minima spanning HJD 2455850–2461007 (2011–2025). O–C diagrams computed using published linear ephemerides from major catalogues reveal systematic parabolic trends, demonstrating that the orbital period is not constant. A global quadratic ephemeris was derived from an unweighted least-squares fit to the complete minima set. The quadratic term corresponds to a secular period decrease of -0.0594 ± 0.0003 s yr^{-1}. Application of the quadratic solution removes the systematic curvature in the O–C residuals over the full baseline. Independent ZTF g-band survey photometry confirms the eclipsing-binary morphology but does not by itself constrain the secular period change. The results demonstrate that previously published linear periods represent local approximations and that V804 And exhibits a small but significant long-term orbital period decrease.

1. Introduction

V804 And (= MoV99) is an eclipsing binary of EB type that was first reported as a variable star by Vrastak [1]. The system was subsequently monitored within the BAV CCD observing programme, where it received the internal designation MoV99. Since its discovery, linear orbital periods for the system have been published in the literature on the basis of data from several large surveys and catalogues, including VSX [2], ASAS-SN [3], ATLAS [4], ZTF [5, 6], and Gaia DR3 [7]. These values agree within their respective uncertainties but are derived from different time windows.

Linear ephemerides determined from restricted observational intervals implicitly assume a constant orbital period. However, long-term eclipse timing of close binaries frequently reveals secular period variations, often attributed to mass transfer, angular-momentum loss, or evolutionary effects. Detecting such changes requires a homogeneous compilation of eclipse timings over an extended temporal baseline.

In this work, we combine all available CCD times of primary and secondary minima obtained between 2011 and 2025 to investigate the long-term timing behaviour of V804 And. By constructing O–C diagrams using published linear elements and by deriving a global quadratic ephemeris, we test whether the orbital period remains constant or exhibits measurable secular evolution.

Observations
400 mm ASA Astrograph f/3.7 - f = 1471 mm, FLI Proline 16803 CCD-Camera - V-filter - t = 120 sec.
Wolfgang Moschner, Astrocamp/Nerpio, Spain

Data analysis
MuniWin [8] and the self-written programs liku2 (Franz Agerer) and StarCurve (Lienhard Pagel) were used for the analysis of the frames after bias, dark, and flat-field correction. The weighted average of five comparison stars was applied.

Explanations:

HJD = heliocentric UTC timings (JD) of the observed minima
All coordinates are taken from the Gaia DR3 catalogue [7]. The coordinates (epoch J2000) are computed by VizieR, and are not part of the original data from Gaia (note that the coordinates are computed from the positions and the proper motions).

V804 And = MoV99

Cross-IDs

= ASASSN-V J021019.10+464044.4
= ATO J032.5795+46.6788
= Gaia DR3 353392765270977280
= UCAC3 274-028753
= ZTF J021019.08+464043.8
= 2MASS J02101909+4640437
= SvkV37
= USNO-B1.0 1366-00046496

Gaia DR3 catalogue:

Right ascension: 02h10m19.0918s at Epoch J2000
Declination: +46° 40' 43.726" at Epoch J2000
14.1007 mag G-band mean magnitude (350-1000 nm)
14.4494 mag Integrated BP mean magnitude (330-680 nm)
13.5735 mag Integrated RP mean magnitude (640-1000 nm)
0.8759 mag BP-RP

Periods known so far:

VSX [2]	0.382973 d	ZTF r-band [5, 6]	0.3829698 d
ASAS-SN [3]	0.3829721 d	ATLAS [4]	0.382972 d
ZTF g-band [5, 6]	0.3829572 d	GCVS 5.1 [9]	0.382973 d
Gaia DR3 [7]	0.38297378 d		

Results

All available primary and secondary CCD times of minima of V804 And (= MoV99) were compiled to establish a homogeneous timing baseline. The CCD minima set used for the ephemeris fit comprises 67 timings (Table 1) spanning HJD 2455850.3151–2461007.4134 (2011–2025). Secondary minima were handled consistently by adopting a phase offset of 0.5 cycles. A single global quadratic ephemeris was derived from an unweighted least-squares fit to the full minima set:

Min. I = HJD 2457748.34036(36) + 0.38297301(12)·E − 3.604(19)×10⁻¹⁰·E²

The negative quadratic coefficient corresponds to a secular period decrease. For the quadratic ephemeris $T(E) = T_0 + P_0E + cE^2$ (with c the quadratic coefficient), differentiation yields $P(E) = dT/dE = P_0 + 2cE$ and, to first order, $\dot{P} = (dP/dE)(dE/dt) \approx 2c/P_0$. Using this relation, we obtain $\dot{P} = (-1.882 \pm 0.010)\times10^{-9}$ d d^{-1}, equivalent to -0.0594 ± 0.0003 s yr^{-1}. The characteristic timescale is $P/|\dot{P}| \approx 5.6\times10^5$ yr. The magnitude of the measured secular period-change rate ($|\dot{P}| \approx 10^{-9}$ d d^{-1}) is in line with values discussed for close / interacting eclipsing binaries in the context of mass transfer and angular-momentum loss (e.g. [10]).

For comparison, O–C residuals were also computed with respect to published linear ephemerides, including linear elements compiled by Kreiner [11]. Published linear ephemerides from VSX [2], ATLAS [4], ASAS-SN [3], the GCVS catalogue [9], and Gaia DR3 variability processing [7] produce systematic O–C trends, including clear curvature over the full baseline, in the corresponding diagrams (Figures 1–6), demonstrating

that constant-period solutions derived from limited survey windows provide only local approximations. When the global quadratic ephemeris is applied, the O–C residuals become nearly flat and symmetrically distributed around zero over the full baseline (Figure 7). As an additional consistency check, Figure 8 shows the phased CCD light curve obtained in Johnson V from CCD observations acquired by the authors over HJD 2457387–2458124 using the global quadratic ephemeris, which illustrates the typical morphology of an eclipsing binary star, characterized by two distinct types of minima.

To validate the timing solution against independent photometric material, ZTF g-band survey photometry was analysed. The ZTF data set contains 421 g-band measurements spanning HJD 2458273.9775–2460609.7645 (2018–2024), with magnitudes ranging from g = 14.298 to 15.040 mag (⟨g⟩ = 14.542, σ = 0.157 mag). Figure 9 presents the ZTF g-band survey photometry as a time-resolved HJD–magnitude distribution, illustrating the long-term temporal coverage of the observations. The photometric scatter (σ = 0.157 mag) is much larger than the typical single-epoch measurement uncertainties of the dataset (≈ 0.02 mag) and is dominated by orbital variability together with survey cadence and sampling. Figure 10 shows the same ZTF data phase-folded with the global quadratic ephemeris, further confirming the validity of the quadratic solution, as the light curve aligns consistently and without systematic phase offsets over the full time span.

Summary on uncertainties

The quadratic ephemeris was obtained from an unweighted fit because the compiled minima timings do not provide homogeneous formal errors. Quoted parameter errors are therefore formal covariance-matrix uncertainties and may underestimate systematics (timing methodology, time-system conventions, and the treatment of secondary minima). Nevertheless, the negative quadratic term ($c < 0$) and hence the secular period decrease are robust, as the parabolic curvature seen with independent linear ephemerides (Figures 1–6) is removed by the quadratic solution (Figure 7). For background on the O–C formalism and common sources of systematic timing errors see Sterken [12].

V804 And = MoV99 calculated with quadratic ephemeris (Bernhard 2026)

Type = EB

Min. I = HJD 2457748.34036(36) + 0.38297301(12)·E − 3.604(19)×10⁻¹⁰·E²

Observer	HJD-Date Minimum	Type	Epoch	O-C (d)	Source
F. Agerer	2455850.3151	I	-4956	-0.0022	
F. Agerer	2455850.5114	II	-4955.5	0.0026	
M. Vrastak	2456155.5465	I	-4159	-0.0029	OEJV169
M. Vrastak	2456157.4629	I	-4154	-0.0014	OEJV169
M. Vrastak	2456898.3316	II	-2219.5	0.0016	OEJV169
M. Vrastak	2456898.5230	I	-2219	0.0016	OEJV169
M. Vrastak	2456930.5031	II	-2135.5	0.0033	OEJV169
Moschner/Frank	2456987.3738	I	-1987	0.0022	
W. Moschner	2457389.3054	II	-937.5	0.0026	
F. Agerer	2457658.3410	I	-235	-0.0007	
F. Agerer	2457658.5351	II	-234.5	0.0019	
W. Moschner	2457693.5752	I	-143	0.0000	
W. Moschner	2457694.5322	II	-140.5	-0.0004	
W. Moschner	2457710.6163	II	-98.5	-0.0012	
W. Moschner	2457712.5322	II	-93.5	-0.0002	
W. Moschner	2457733.4010	I	-39	-0.0034	
W. Moschner	2457748.3392	I	0	-0.0012	
W. Moschner	2457759.4471	I	29	0.0005	
W. Moschner	2458017.5705	I	703	0.0003	
W. Moschner	2458029.6386	II	734.5	0.0048	
W. Moschner	2458042.6556	II	768.5	0.0007	
W. Moschner	2458078.4618	I	862	-0.0010	
W. Moschner	2458080.3770	I	867	-0.0007	

W. Moschner	**2458112.3589**	**II**	**950.5**	**0.0030**	
W. Moschner	**2458124.4152**	**I**	**982**	**-0.0043**	
W. Moschner	**2458384.6508**	**II**	**1661.5**	**0.0018**	
W. Moschner	**2458434.4355**	**II**	**1791.5**	**0.0002**	
W. Moschner	**2458434.6244**	**I**	**1792**	**-0.0024**	
W. Moschner	**2458730.6592**	**I**	**2565**	**-0.0046**	
W. Moschner	**2458750.5768**	**I**	**2617**	**-0.0015**	
W. Moschner	**2458759.5816**	**II**	**2640.5**	**0.0035**	
W. Moschner	**2458766.6611**	**I**	**2659**	**-0.0019**	
W. Moschner	**2458815.2976**	**I**	**2786**	**-0.0028**	
W. Moschner	**2458815.4931**	**II**	**2786.5**	**0.0012**	
W. Moschner	**2458818.3621**	**I**	**2794**	**-0.0020**	
W. Moschner	**2458829.4703**	**I**	**2823**	**0.0000**	
W. Moschner	**2458857.4259**	**I**	**2896**	**-0.0013**	
W. Moschner	**2459103.6764**	**I**	**3539**	**-0.0009**	
W. Moschner	**2459119.5702**	**II**	**3580.5**	**-0.0004**	
W. Moschner	**2459129.5288**	**II**	**3606.5**	**0.0009**	
W. Moschner	**2459129.7178**	**I**	**3607**	**-0.0015**	
W. Moschner	**2459150.5907**	**II**	**3661.5**	**-0.0005**	
W. Moschner	**2459156.5263**	**I**	**3677**	**-0.0009**	
W. Moschner	**2459177.3993**	**II**	**3731.5**	**0.0002**	
W. Moschner	**2459199.4197**	**I**	**3789**	**-0.0002**	
W. Moschner	**2459446.6306**	**II**	**4434.5**	**0.0035**	
W. Moschner	**2459455.6251**	**I**	**4458**	**-0.0018**	
W. Moschner	**2459580.2829**	**II**	**4783.5**	**-0.0006**	
W. Moschner	**2459806.6200**	**II**	**5374.5**	**0.0016**	
W. Moschner	**2459827.6820**	**II**	**5429.5**	**0.0003**	
W. Moschner	**2459854.6817**	**I**	**5500**	**0.0007**	
W. Moschner	**2459883.5975**	**II**	**5575.5**	**0.0023**	
W. Moschner	**2459933.3837**	**II**	**5705.5**	**0.0025**	
W. Moschner	**2460214.4847**	**II**	**6439.5**	**0.0046**	
W. Moschner	**2460229.6065**	**I**	**6479**	**-0.0008**	
W. Moschner	**2460274.4155**	**I**	**6596**	**0.0008**	
W. Moschner	**2460289.3473**	**I**	**6635**	**-0.0031**	
W. Moschner	**2460297.3931**	**I**	**6656**	**0.0003**	
W. Moschner	**2460577.5323**	**II**	**7387.5**	**-0.0015**	
W. Moschner	**2460635.3632**	**II**	**7538.5**	**0.0013**	
W. Moschner	**2460645.3205**	**II**	**7564.5**	**0.0014**	
W. Moschner	**2460660.4442**	**I**	**7604**	**-0.0021**	
W. Moschner	**2460669.2541**	**I**	**7627**	**-0.0005**	
W. Moschner	**2460685.3390**	**I**	**7669**	**-0.0002**	
W. Moschner	**2460974.4786**	**I**	**8424**	**-0.0008**	
W. Moschner	**2461001.2879**	**I**	**8494**	**0.0008**	
W. Moschner	**2461007.4134**	**I**	**8510**	**-0.0012**	

Table 1: Minima of V804 And = MoV99 calculated with quadratic ephemeris (Bernhard 2026).
The O-C of the secondary minima were calculated assuming that the true phase is exactly at 0.5. Numbers in parentheses denote the formal 1σ uncertainty in the last digits

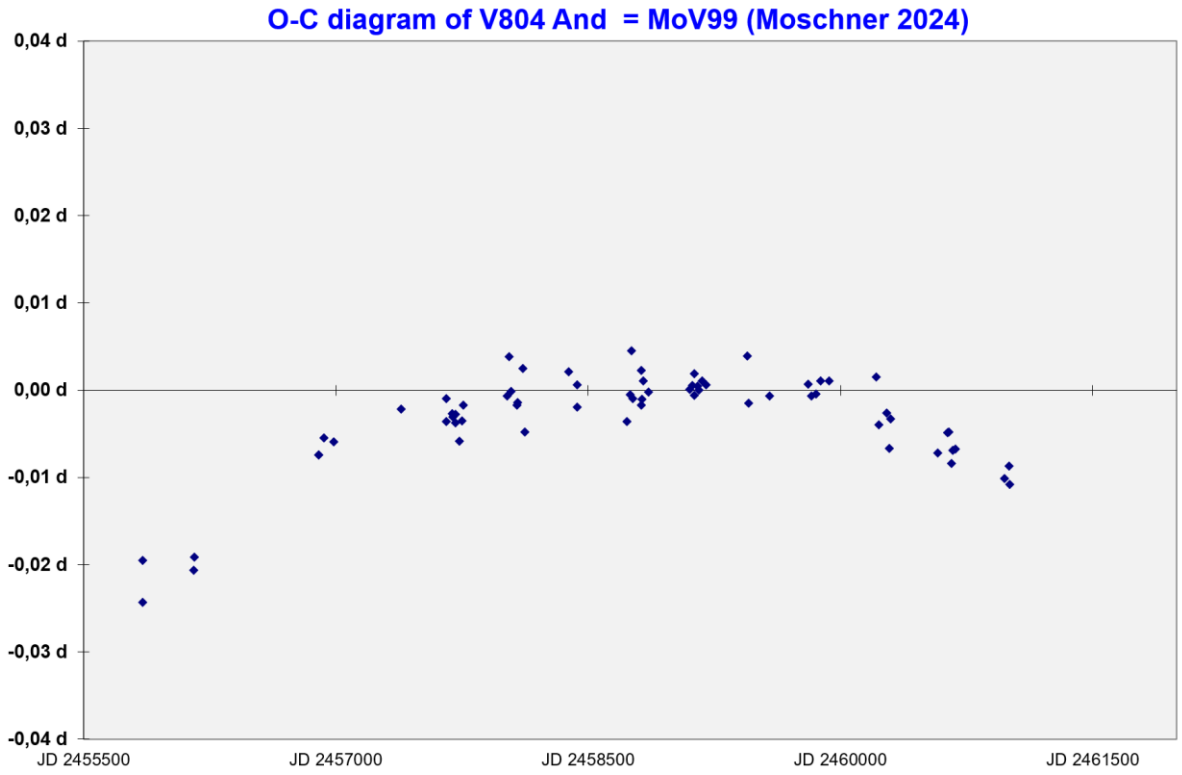

Figure 1: O–C diagram computed using a linear ephemeris fitted to the late CCD-minima subset (2022–2023), i.e. a local constant-period approximation. The resulting curvature demonstrates that a restricted-interval linear ephemeris cannot reproduce the full-baseline timing behaviour.

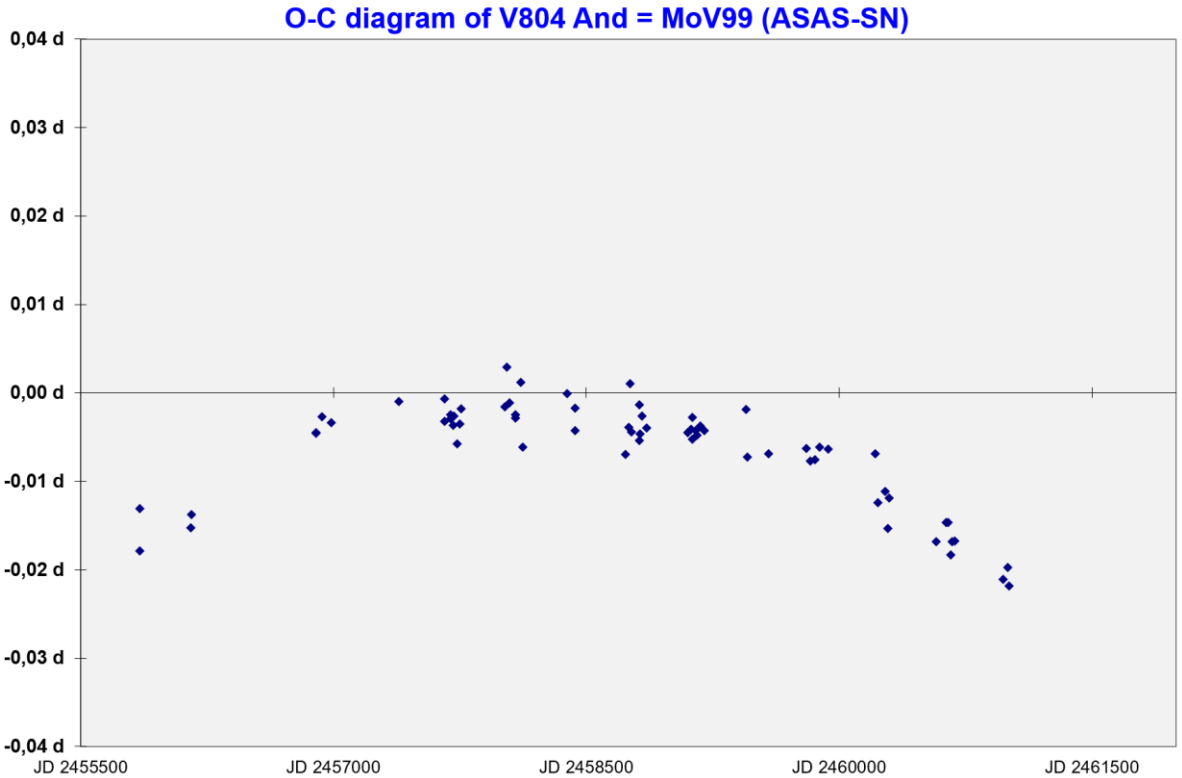

Figure 2: O–C diagram computed using a linear ephemeris representative of the early CCD-minima subset (2018–2021; close to the ASAS-SN catalogue period). The systematic curvature differs from Figure 1, illustrating that linear periods obtained from different time windows are mutually inconsistent in the presence of secular evolution.

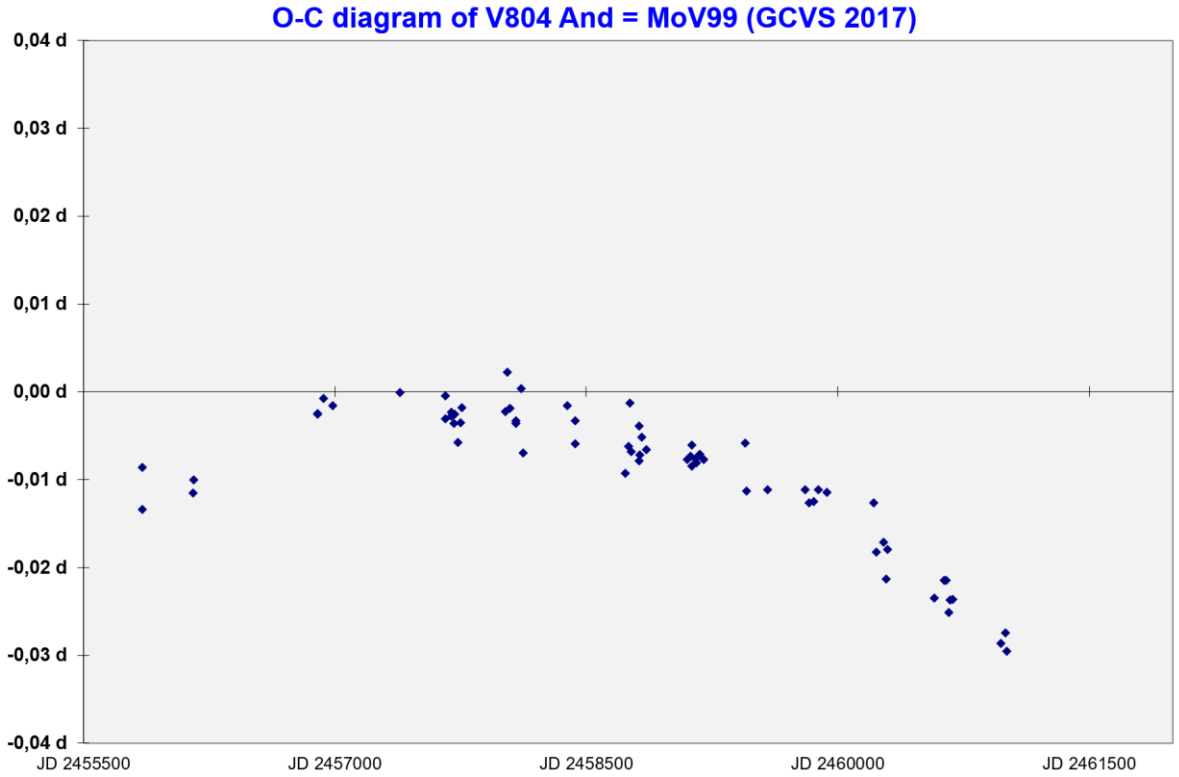

Figure 3: O–C diagram computed using linear ephemeris elements adopted from the GCVS 2017 / GCVS 5.1 catalogue [9] (period consistent with the value listed in VSX [2]). The parabolic trend reflects the non-constant orbital period and is consistent with a secular period decrease.

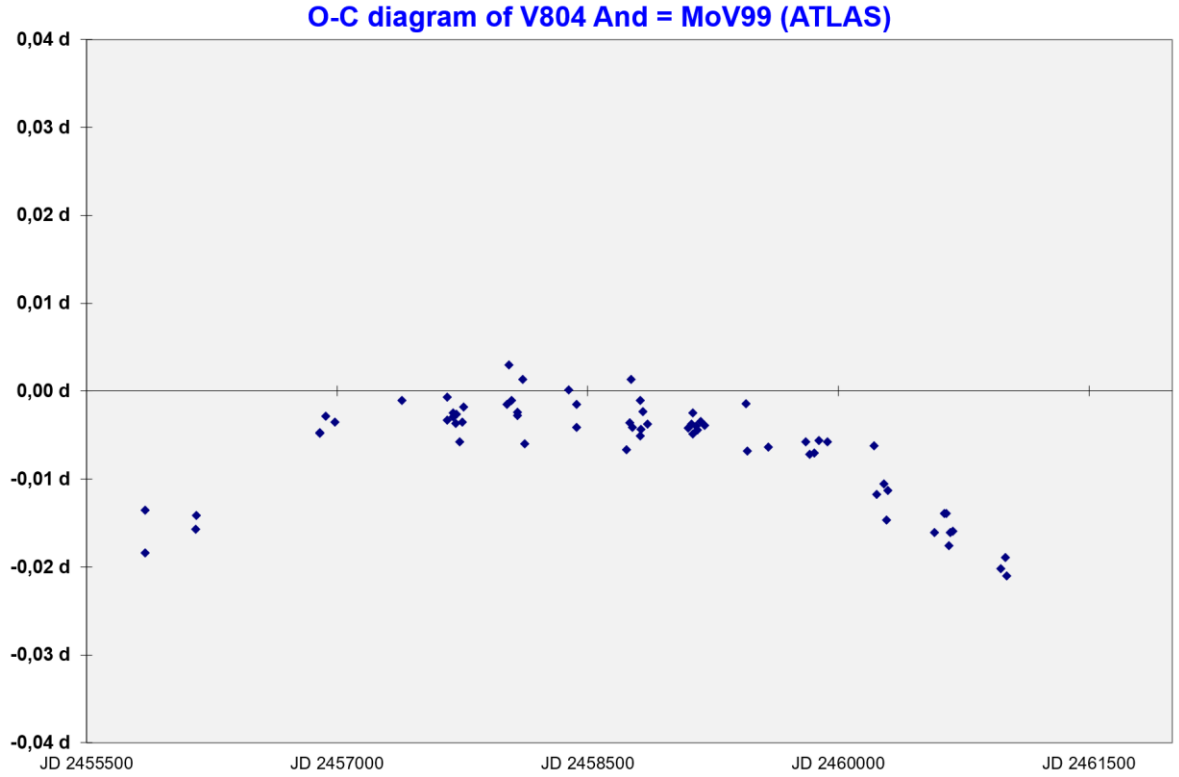

Figure 4: O–C diagram computed using the linear period published by the ATLAS survey [4]. The systematic deviation from zero indicates that the ATLAS period represents an effective mean value over its observational window.

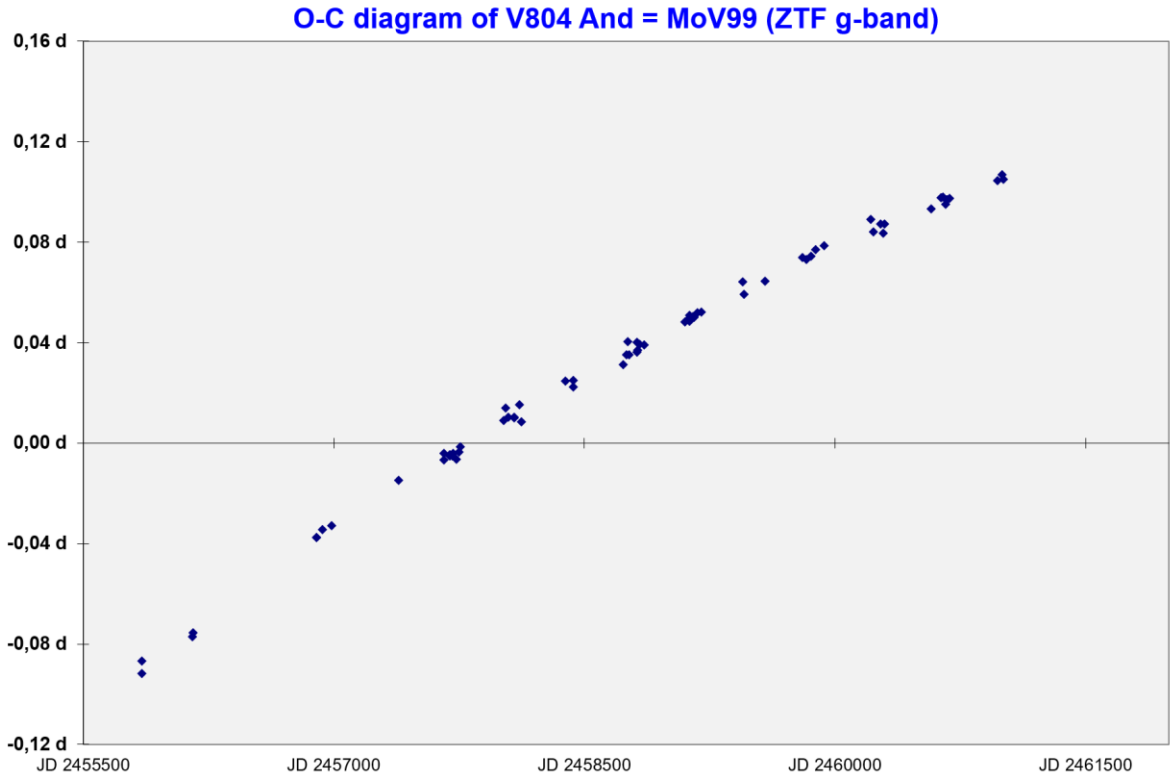

Figure 5: O–C diagram computed using the linear period adopted from the ZTF periodic variable-star catalogue [6], based on ZTF survey photometry [5]. The O–C diagram shows a strong systematic, approximately linear drift, indicating that the ZTF g-band period represents an effective mean over the ZTF time window and is offset with respect to the long-baseline ephemeris.

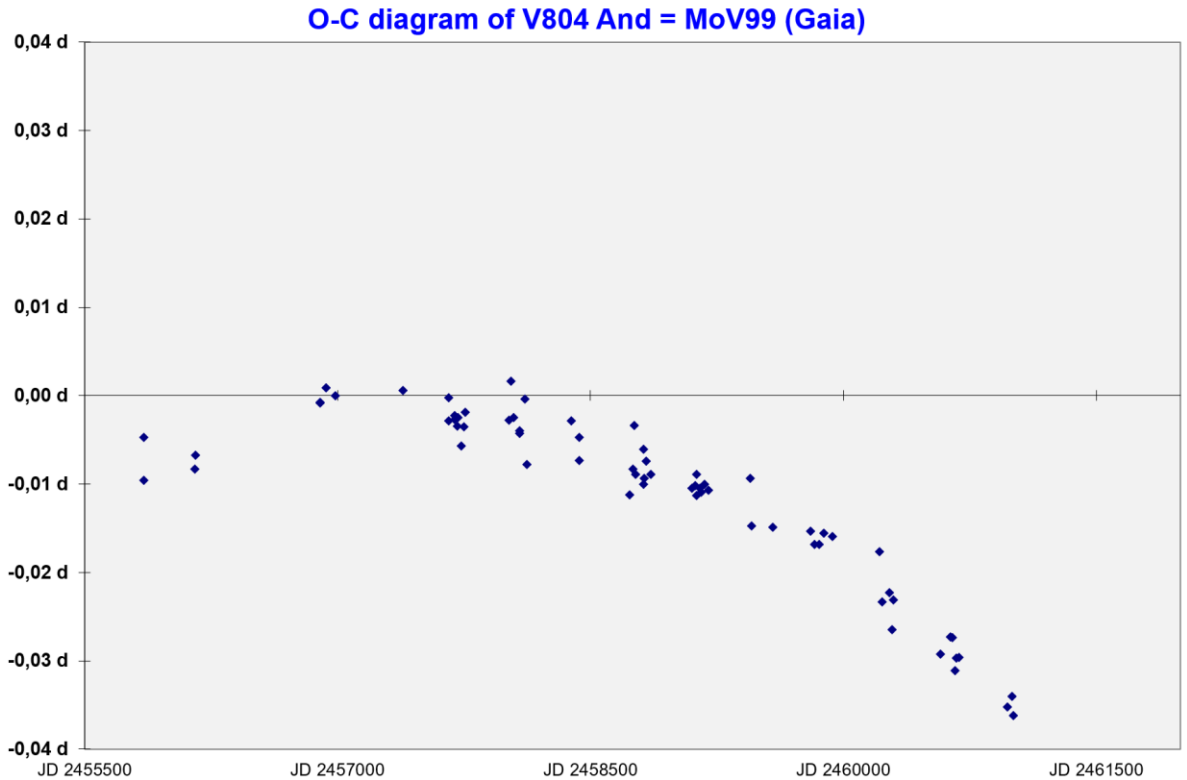

Figure 6: O–C diagram computed using the linear period from Gaia DR3 variability processing [7]. The observed systematic trend provides independent evidence for a non-constant orbital period.

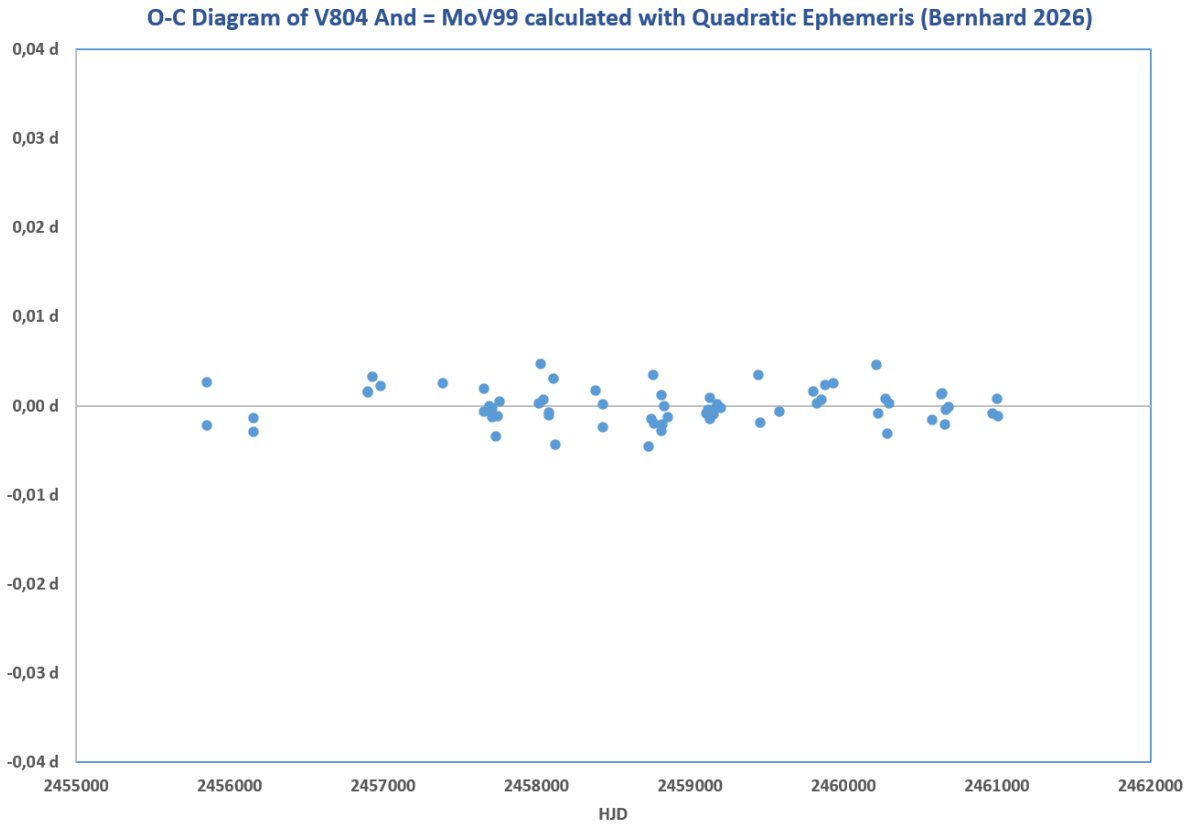

Figure 7: O–C residuals of V804 And (= MoV99) with respect to the global quadratic ephemeris (Table 1). The residuals show no remaining systematic curvature, indicating that the quadratic solution provides an adequate description of the long-term timing behaviour.

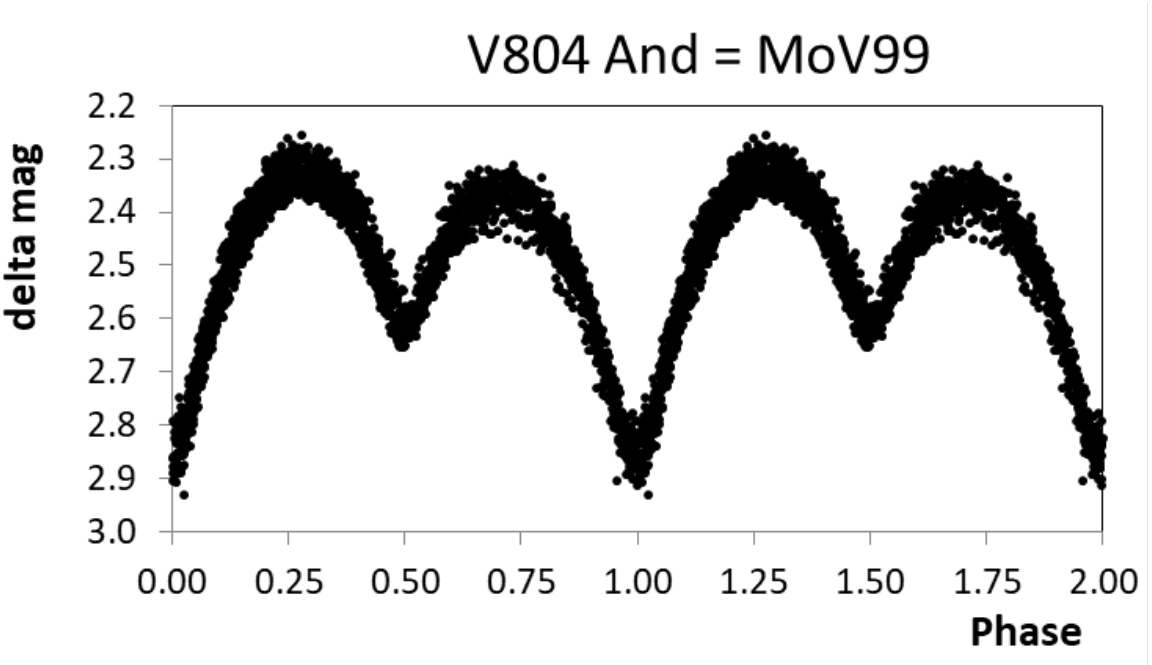

Figure 8: Phased CCD light curve of V804 And = MoV99 obtained in Johnson V from CCD observations of the authors acquired over HJD 2457387–2458124 and phase-folded using the global quadratic ephemeris.

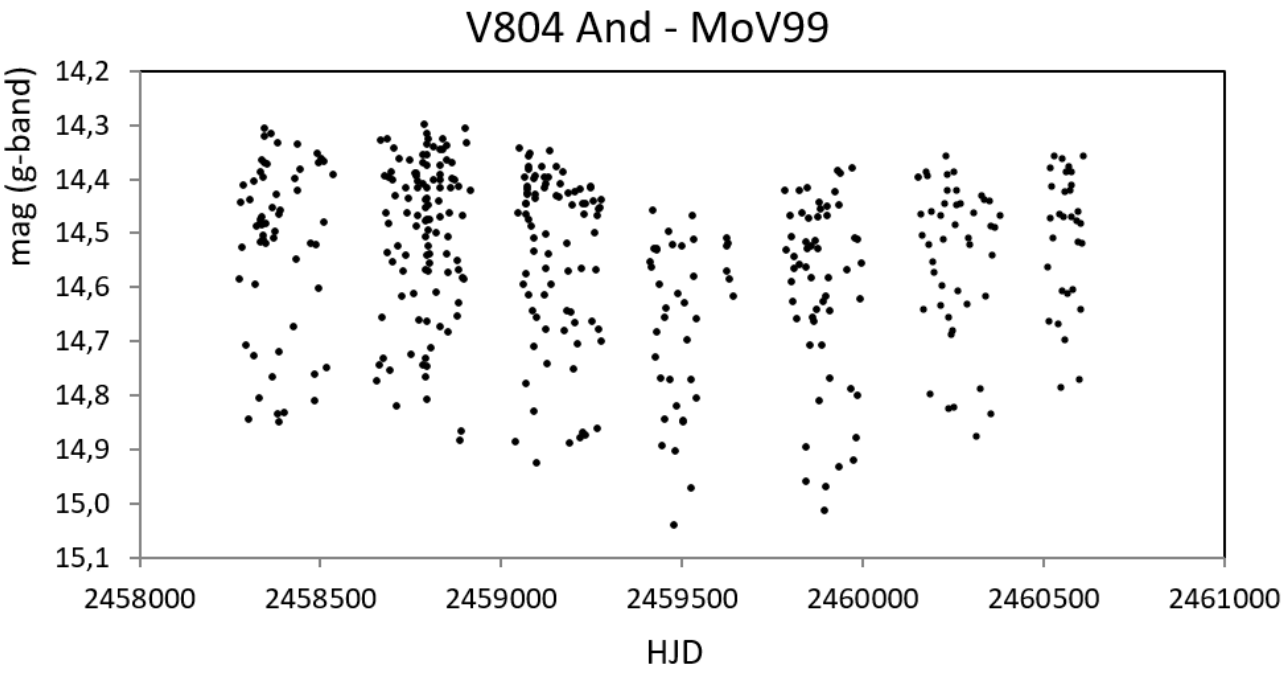

Figure 9: ZTF g-band survey photometry of V804 And (= MoV99) plotted as a function of heliocentric Julian date (HJD). The time-resolved distribution illustrates the long-term survey coverage and the observed photometric scatter, which reflects the combination of orbital variability and survey sampling; quantifying any long-term change in mean out-of-eclipse brightness requires phase-filtered diagnostics.

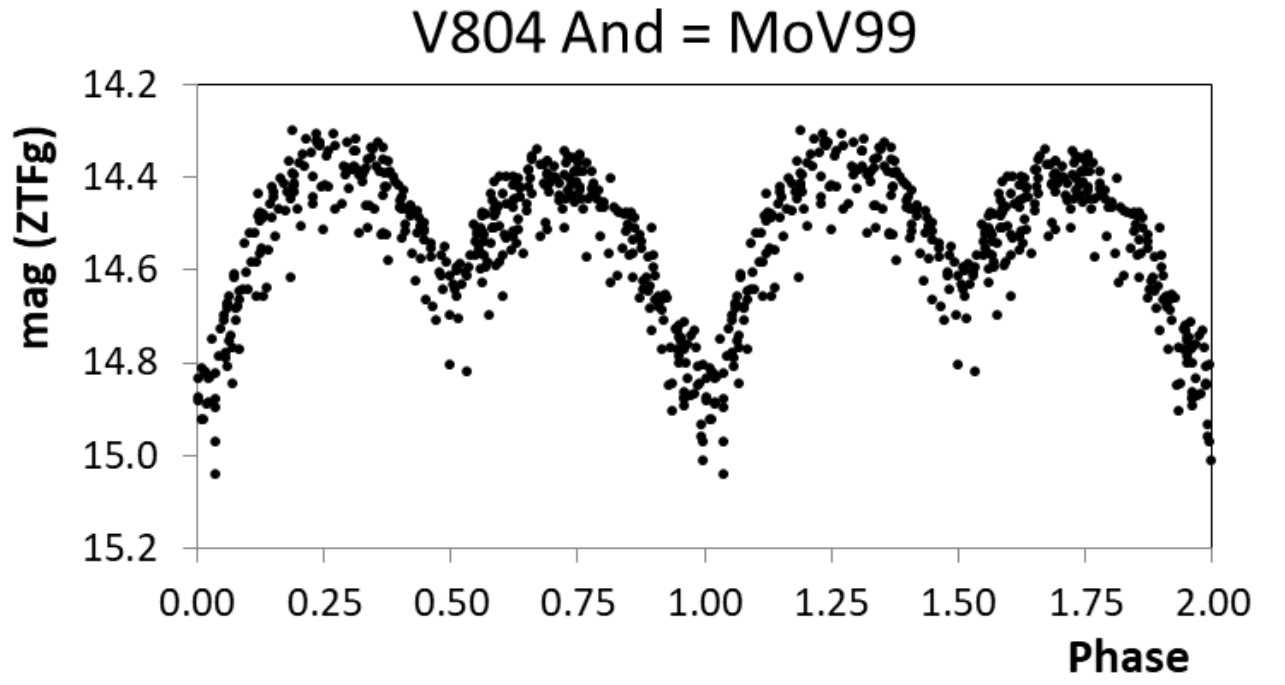

Figure 10: Phase-folded ZTF g-band light curve of V804 And (= MoV99) using the global quadratic ephemeris

Acknowledgements

This research has made use of the SIMBAD database [13], operated at CDS, Strasbourg, France, the International Variable Star Index (VSX) database, operated at AAVSO, Cambridge, Massachusetts, USA, the Gaia Project, operated by European Space Agency, the ATLAS-Project developed by the University of Hawaii and funded by NASA, the ZTF-Project, operations are conducted by COO, IPAC and University of Washington.

The authors thank David Motl for providing his MuniWin photometry program, Franz Agerer (BAV) for providing his data analysis program liku2, and Lienhard Pagel (BAV) for providing his data analysis program StarCurve [14].

References

[1] Vrastak, M., 2015, New Variable Stars in SvkV Catalogue, Open European Journal on Variable Stars, 169, 23.

https://ui.adsabs.harvard.edu/abs/2015OEJV..169...23V/abstract

[2] Watson, C. L., Henden, A. A., Price, A., 2006, The International Variable Star Index (VSX).

https://vsx.aavso.org/index.php?view=detail.top&oid=476420

[3] Jayasinghe, T., et al., 2018, The ASAS-SN Catalog of Variable Stars I: The Serendipitous Survey, MNRAS, 477, 3145.

https://ui.adsabs.harvard.edu/abs/2018MNRAS.477.3145J/abstract
https://asas-sn.osu.edu/variables/fd74fe48-973a-59fe-982d-51ea4cb0f9a7

[4] Heinze, A. N., et al., 2018, A First Catalog of Variable Stars Measured by ATLAS, AJ, 156, 241.

https://ui.adsabs.harvard.edu/abs/2018AJ....156..241H/abstract
https://cdsarc.u-strasbg.fr/viz-bin/cat/J/AJ/156/241

[5] Bellm, E. C., et al., 2019, The Zwicky Transient Facility: System Overview, PASP, 131, 018002.

https://ui.adsabs.harvard.edu/abs/2019PASP..131a8002B/abstract

[6] Chen, X., Wang, S., Deng, L., de Grijs, R., Yang, M., Tian, H., 2020, The Zwicky Transient Facility Catalog of Periodic Variable Stars, ApJS, 249, 18.

https://ui.adsabs.harvard.edu/abs/2020ApJS..249...18C/abstract
https://cdsarc.u-strasbg.fr/viz-bin/cat/J/ApJS/249/18

[7] Eyer, L., et al., 2023, Gaia Data Release 3: Summary of the variability processing and analysis, A&A, 674, A13.

https://ui.adsabs.harvard.edu/abs/2023A%26A...674A..13E/abstract
https://cdsarc.u-strasbg.fr/viz-bin/cat/I/358

[8] Munipack and C-Muniwin software. Source code and binaries.

http://c-munipack.sourceforge.net

[9] Samus, N. N.; Kazarovets, E. V.; Durlevich, O. V.; Kireeva, N. N.; Pastukhova, E. N., 2017, General Catalogue of Variable Stars: Version GCVS 5.1, Astronomy Reports, 61, 80–88.

https://ui.adsabs.harvard.edu/abs/2017ARep...61...80S/abstract
http://www.sai.msu.su/gcvs/cgi-bin/search2.cgi?search=V804+And

[10] Sargsyan, V. V., Lenske, H., Adamian, G. G., Antonenko, N. V., 2019, Origin of the orbital period change in contact binary stars, Int. J. Mod. Phys. E, 28, 1950044.

https://www.worldscientific.com/doi/full/10.1142/S0218301319500447
https://ui.adsabs.harvard.edu/abs/2019IJMPE..2850044S/abstract

[11] Kreiner, J. M., 2004, Up-to-date linear elements of eclipsing binaries, Acta Astronomica, 54, 207.

https://ui.adsabs.harvard.edu/abs/2004AcA....54..207K/abstract

[12] Sterken, C., 2005, The O–C Diagram: Basic Procedures, ASP Conf. Ser., 335, 3.

https://ui.adsabs.harvard.edu/abs/2005ASPC..335....3S/abstract

[13] Wenger, M., et al., 2000, The SIMBAD astronomical database, A&AS, 143, 9.

https://ui.adsabs.harvard.edu/abs/2000A%26AS..143....9W/abstract
https://simbad.cds.unistra.fr/simbad/sim-id?Ident=V804+And

[14] StarCurve software package (BAV tutorial pages).

https://www.bav-astro.eu/index.php/weiterbildung/tutorials